Pol. J. Environ. Stud. Vol. XX, No. X (XXXX), 1-18
DOI: 10.15244/pjoes/237573 ONLINE PUBLICATION DATE: 2026-11-16

Original Research

Ozone and Thermal Comfort Responses in Signature Urban Microenvironments under Non-typical Weather

Yuping Jiang[1]*, Yifeng Jiang[2], Shimin Wu[1], Jieying Han[1], Fulan Wang[1]

[1]University of Electronic Science and Technology of China, Zhongshan Institute, Zhongshan City, 512000, Guangdong Province, China
[2]Changsha University of Science & Technology, School of Materials Science and Engineering - Yuntang Campus, Changsha City, 410114, Hunan Province, China

Received: 29 April 2026
Accepted: 20 September 2026

Abstract

Urban street microenvironments exhibit pronounced heterogeneity in both physical morphology and anthropogenic activity, but ozone pollution and heat stress during non-typical meteorological periods remain poorly understood in these microenvironments. To address this research gap, this study focused on the representativeness of thermal environment and pollution effects, for which two contrasting microenvironments were selected: (I) an "urban desertification" area dominated by impervious surfaces, and (II) a "traffic-dining" composite pollution belt. Using KZ filtering, regression, and GAM, we found that short-term fluctuations account for over 77% of total O_3 variance in both areas, with wind speed emerging as a key suppressor of O_3 at sub-hourly scales. At longer timescales, solar radiation and temperature positively correlate with O_3, while humidity exerts a negative influence – effects more pronounced in the traffic-dining zone. GAM analysis reveals strong nonlinear relationships between meteorological factors and O_3. The meteorological factors exhibit varying degrees of correlation and jointly regulate both O_3 and Wet Bulb Globe Temperature (WBGT), thereby revealing for the first time a compensatory mechanism between the two indices. This study highlights the need for fine-scale, high-frequency monitoring to improve microenvironment management and urban livability.

Keywords: meteorological factors, ozone, Wet Bulb Globe Temperature (WBGT), coordination, effect

Introduction

With the deepening of urbanization, the highly artificial nature of urban underlying surfaces (such as dense buildings and impervious pavements) and the concentration of human activities (such as traffic flow and restaurant emissions) collectively shape a microscale meteorological environment with significant heterogeneity [1, 2]. It encompasses both specific physical elements like streets, green spaces, and buildings, as well as social behavioral characteristics such as communities and traffic, and fluctuates rapidly

*e-mail: jyp@zsc.edu.cn
Tel.: +86 760 88325742
Fax: +86 760 88325742
0000-0003-2538-973X

© 2026 This article is licensed under a Creative Commons Attribution-NonCommercial 4.0 International (CC BY-NC 4.0)

with time (season, day) [3]. These microenvironments are much smaller in scale than the urban environments or even neighborhood environments studied in general research, yet they can form anomalous "microclimates" within a small range [4]. They not only alter the spatiotemporal distribution characteristics of local temperature, humidity, solar radiation, and wind speed [5], but also play a critical regulatory role in the formation and evolution of ground-level ozone (O_3). Furthermore, ozone can interact with heat stress to form compound extreme weather events [6, 7], which further amplifies potential risks to human health, making this a significant bottleneck constraining the quality of the urban living environment. Currently, the academic community has accumulated a substantial body of research on the relationships among meteorological factors, ozone, and thermal environment indicators, but there are four main shortcomings. First, research has predominantly focused on large scales while neglecting the microenvironment scale. However, the coarse resolution of large-scale climate data does not align with the microclimate actually experienced by organisms, such as temperature buffering for montane forests [8], especially since the link between microclimate and the microenvironment is inherently tight [9]. In this context, urban street canyons represent a critical type of microenvironment, serving as key hotspots for both heat stress and traffic-related pollutants [10]. Second, there is an emphasis on analyzing the driving effects of large-scale meteorological fields (such as monsoon circulation and subtropical highs) on ozone during hot and humid periods, while overlooking the distinct characteristics of microenvironments in non-hot, non-humid seasons. Although these periods do not meet the traditional "hot and humid" conditions associated with high ozone occurrence, they may still exhibit atypical patterns of ozone concentration due to intensified local emissions (e.g., favorable weather leading to increased traffic-related NO_x and cooking-related VOC emissions), coupled with non-negligible meteorological conditions. Third, fluctuations in ozone concentration may be influenced by factors at annual, seasonal, and diurnal scales [11, 12], but they may also be driven by more refined, minute-level meteorological perturbations (such as gusts) or hourly variations in traffic, commuting patterns, and meteorological trends (like gradual temperature increases). These fine temporal scales often align with the duration of time people spend outdoors in microenvironments; however, existing research has not yet addressed this aspect. Fourth, thermal comfort is also influenced by changes in meteorological conditions. For instance, since the radiative effects differ significantly between daytime and nighttime, they need to be considered separately to improve thermal comfort [13]. In fact, even daytime meteorological conditions can change abruptly, affecting thermal comfort. Therefore, thermal environment indicators and ozone pollution share common influencing factors. However, research on the relationship between the two remains fragmented, with few studies exploring their intrinsic connections or the compensatory mechanisms that could yield mutual benefits. This gap hinders the development of microenvironment management strategies that synergistically address both "pollution control and thermal comfort optimization." While this study cannot fully address the aforementioned research gaps, it strives to target these shortcomings for focused and innovative exploration.

Therefore, this study proposes two core hypotheses. First, even during non-typical hot and humid meteorological periods, meteorological factors (temperature, humidity, radiation, wind speed) exert differentiated impacts on ozone concentrations within urban street micro-morphologies and microenvironments characterized by varying socioeconomic backgrounds, and these influences exhibit multi-temporal scale characteristics. Second, although the thermal environment indicator (WBGT) and ozone concentration belong to different environmental assessment categories, they are potentially linked because they are both regulated by meteorological factors. Utilizing this linkage allows for the identification of compensatory mechanisms that can simultaneously meet the requirements of both indicators.

Field monitoring for this study was conducted in Zhongshan City, located in the southern subtropical monsoon climate zone. The climate of this region is characterized by high temperatures, high humidity, abundant rainfall, and strong solar radiation during summer, which constitute typical meteorological conditions for the formation and accumulation of ground-level ozone (O_3). In contrast, the monitoring period selected for this study featured clear and stagnant weather, with significantly lower temperatures, humidity, and solar radiation compared to summer conditions. Additionally, traffic and dining-related emissions during this period differed from those in the typical ozone season. These conditions define the "non-typical weather" as delineated in our work. Impervious surface area is a critical parameter for characterizing the thermal environment [14], and VOCs emitted from cooking activities contribute significantly to urban ozone (O_3) formation from a chemical perspective [15]. Kazemi et al. also found that the proportion of impervious surfaces and traffic emissions are key factors driving the patterns of the thermal environment and pollution [16], respectively, with their spatial distributions exhibiting both independence and interaction. Therefore, this study selects two typical urban microenvironments as representative case studies. The first is characterized by a high proportion of impervious surfaces, creating an "urban desertification" thermal environment with intense surface longwave radiation reflection (Monitoring Area I). The second is a "traffic-dining" composite pollution zone affected by the combined influence of traffic emissions and cooking fumes (Monitoring Area II). The study conducted field monitoring during a non-hot, non-humid meteorological

period, simultaneously collecting data on ozone concentration, meteorological factors (air temperature, relative humidity, solar radiation intensity, wind speed), and thermal environment indicators (Wet-Bulb Globe Temperature, WBGT). This approach aimed to decompose the ozone concentration time series, analyze the relationships between meteorological factors and ozone, and identify compensatory regulatory patterns of meteorological factors under consistent indicator conditions.

Materials and Methods

Instrument

The instruments used in the present study are detailed in Table 1.

Experiment

Selection of Monitoring Areas

Monitoring was conducted on clear afternoons (14:00-17:00, a period of active solar radiation and ozone photochemical reactions) from December 20 to 30, 2024. The typical meteorological conditions during this period differed from the hot and humid conditions of summer and autumn, with an average temperature of 21°C, northeast winds at speeds <2 m/s, and an average relative humidity of 65%. Monitoring included two areas (as shown in Fig. 1). Monitoring Area Ⅰ is adjacent to a major traffic artery, representing a typical high-density built-up area with intense surface longwave radiation reflection, constituting a classic "urban desertification" thermal environment. Monitoring Area Ⅱ is a zone where dining commerce and traffic pollution converge,

Table 1. Instruments.

Instrument	Model	Manufacturer
Pump-suction ozone detector	uSafe 3000-O3-M	Shandun Technology (Shenzhen) Co., Ltd.
Thermal anemometer	DT-3880	Qingdao Lubo Jianye Environmental Technology Co., Ltd.
Radiant heat meter	MR-5	Qingdao Xiecheng Chuangxin Environmental Technology Co., Ltd.
Digital illuminance meter	TES-1332A	Qingdao Jingcheng Instrument Co., Ltd.
Wet Bulb Globe Temperature (WBGT) meter	AZ8778	Shidexin Technology (Shenzhen) Co., Ltd.



Fig. 1. Monitoring areas.

characterized by a linear layout that forms a "road-dining" composite pollution belt.

Monitoring

Data were recorded at 3-minute intervals in accordance with the instrument operating procedures. During monitoring, instruments were positioned at breathing-zone height and placed in direct sunlight. The fundamental environmental parameters monitored included ozone concentration, solar radiation intensity, ambient air temperature, relative humidity, globe temperature, and the WBGT index.

Relationship Analysis

(1) KZ Filtering

KZ filtering is a method that decomposes a time series into components at different scales by utilizing the frequency-domain characteristics of data variation. It involves performing p iterative operations using a moving average window of length m data points until the components at the desired frequency are separated. The calculation formula is as follows:

$$Ys = \frac{1}{m}\sum_{j=-k}^{k} Xs + j \quad (1)$$

Where *Ys* represents the time series after the s-th filtering calculation, m is the total length of the sliding window, k is the length of the sliding window on both ends during filtering, *Xs+j* is the filtered time series, and s is the time interval of the series. The result of each filtering calculation serves as the input for the next filtering step. After p iterative calculations, the final filtering result is obtained. Based on references [17, 18], since the sample data have been arithmetically averaged to reduce "noise" interference to some extent, and to minimize boundary loss (with only 61 sample groups after averaging), a narrow-window KZ filtering method was adopted. The original time series was decomposed as follows:

$$X(t) = B(t)+W(t) \quad (2)$$

where B(t) is the baseline component, with a window length m = 7 and iteration count p = 1, representing cyclical changes over approximately 21 minutes; W(t) is the short-term component, representing random or irregular fluctuations.

(2) Multiple Linear and Ridge Regression

Conventional multiple linear regression analysis essentially expresses the ordinal relationship between dependent and independent variables. It can simultaneously account for the influence of multiple independent variables on the dependent variable, enabling a comprehensive assessment of the relative importance and independence of each factor. This method has been applied to study ozone trends [19] and the relationship between ozone and other environmental variables [20]. Therefore, this study first employs multiple linear regression analysis to model the relationships among factors, capturing the influence of each variable from a holistic and systematic perspective. However, conventional ordinary least squares (OLS) regression is prone to coefficient inflation and distorted significance estimation when strong multicollinearity exists among the independent variables. To address this issue, this study further employs ridge regression to model the relationship between meteorological factors and ozone concentration, following the approach of Omara [21]. By introducing an L2 regularization term into the loss function, this approach shrinks the regression coefficients to mitigate the effects of collinearity, with the optimal ridge parameter λ selected via 10-fold cross-validation.

(3) Least Absolute Deviations (LAD) Regression

To evaluate whether the estimated directions of meteorological driving effects are robust to potential outliers, this study further applies least absolute deviations (LAD) regression, following the approach described in [22]. This method is equivalent to median regression (quantile regression at $\tau = 0.5$). Unlike OLS, which minimizes the sum of squared residuals, LAD minimizes the sum of absolute residuals, thereby reducing the influence of extreme ozone observations. Model performance is summarized using pseudo R^2, MAE, and RMSE, rather than the conventional OLS R^2.

(4) GAM Model Analysis

The GAM is a data-driven, nonparametric regression model. Its primary advantage lies in not requiring predefined assumptions about the parametric relationship between the response and explanatory variables. Instead, it fits smooth functions to the explanatory variables, automatically selecting appropriate polynomial parameters based on the data's own characteristics. This allows it to capture both nonlinear and linear relationships within the data. This study applies the GAM to further explore nonlinear patterns in the data, following the methodology proposed by Boleti et al. [23, 24], as shown in Equation (3):

$$\mu_i = \beta_0 + s_1(temp_i) + s_2(rh_i) + s_3(rad_i) + s_4(wind_i) \quad (3)$$

Where β_0 is the intercept, i represents the i-th observation, and $s_j(.)$ are thin-plate regression spline smooth functions for the independent variables temp, rh, rad, and wind, respectively.

In this study, all smooth terms were fitted using thin-plate regression splines, a widely adopted basis function in air quality and environmental statistics, which offers good numerical stability and avoids arbitrary knot selection. The smoothing parameter λ for each spline term, which governs the wiggliness of the smooth curve and determines the effective degrees of freedom (EDF), was automatically optimized via generalized cross-validation (GCV). This criterion balances

Table 2. Comparison of ozone concentrations across the monitoring areas.

Statistical parameters	Monitoring Area I	Monitoring Area II
	The average O_3 concentration (μg m^{-3})	
mean	184.67	185.28
std	8.58	13.45
min	163.35	163.18
25%	181.52	172.88

in-sample fitting accuracy and model complexity to prevent overfitting and ensure robust generalization performance.

Results and Discussion

Apparent Variation of Ozone

From Table 2, it can be seen that although the average O_3 concentrations in the two areas are at similar levels overall, an analysis of the standard deviation reveals that the fluctuation range and degree of dispersion are greater in Monitoring Area II. This indicates a difference in the micro-environmental conditions between the two areas, with anthropogenic activities likely constituting a significant cause for the more pronounced interference observed in Monitoring Area II.

From the standard deviation results in Table 3, it is evident that ozone is the most unstable indicator, whereas the related meteorological factors are relatively stable. This suggests that even though the variation in meteorological factors during the experimental process was minimal, other influencing factors must be affecting ozone levels, leading to its sharp fluctuations. As ozone is both a prominent pollutant and perceptible to humans [25], its pollution cannot be overlooked, even in this atypical ozone-forming environment.

As shown in Fig. 2, the ozone concentration in Area II shows an increasing trend between 14:00 and 14:30, while it fluctuates sharply in Area I. Between 15:00 and 15:30, the ozone concentrations in both areas fluctuate. After 15:30, the concentration in Area II drops sharply and then continues to fluctuate at a low level, whereas in Area I, it continues to fluctuate with a very slight upward trend. Within the measurement period of this study, some studies have reported continuously increasing ozone concentrations [11] that peak and then decline [26], or have shown significant differences between urban and rural areas [27]. However, these trends were not observed in the present study. The reason for this discrepancy is that such trends are typically identified in large-scale studies, which clearly differ from the small-scale microenvironment examined here. This finding underscores that even within larger spatial and temporal contexts, ozone pollution at a finer scale can still exhibit distinct variations, warranting more detailed investigation.

Influence of Different Time Scales on Ozone

The original O_3 concentration time series from both areas were decomposed into baseline and short-term components using the KZ filter method. Fig. 3 shows that the fluctuations of the baseline component are substantially lower than those of the short-term component, revealing that the variation in O_3 concentration is primarily attributable to the short-term component. In other words, it is driven by the short-term variations of the influencing factors. Further analysis, as presented in Table 4, confirms that the variance contribution of the short-term component is the largest in both areas, at 80.2% and 77.7%, respectively. This indicates that the fluctuations in the O_3 concentration time series are primarily caused by the short-term component, meaning they result from short-term perturbations with periods of less than 21 minutes. Comparing the two areas, the short-term component in area II exhibits relatively greater variation, fluctuating within a range of -22.78 to 14.26 μg m^{-3}. This indicates that O_3 levels in this area are the most significantly affected by short-term perturbations. The baseline component, obtained after noise removal, shows that although the peak O_3 concentrations in the two areas are quite similar, the peak occurs later in area I,

Table 3. Standard deviation of indicators.

Monitoring Area I		Monitoring Area II	
Indicator	Standard deviation	Indicator	Standard deviation
O_3	10.935	O_3	11.752
temp	1.061	temp	0.834
rh	1.612	rh	0.745
rad	0.084	rad	0.094
wind	0.201	wind	0.134
WBGT	1.057	WBGT	0.991

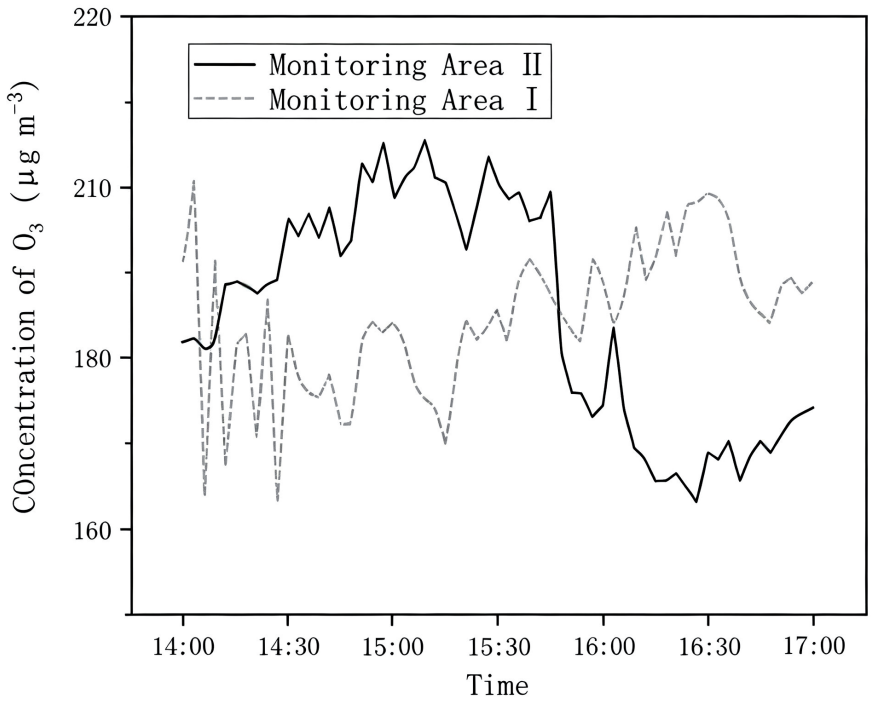


Fig. 2. The relationship between ozone concentration and time.

and the baseline component itself also shows considerable fluctuation there. These differences may be related to variations in pedestrian traffic, transportation, and food service emissions, as well as environmental conditions between the two areas, combined with meteorological factors. This also provides initial confirmation of the first hypothesis: Monitoring Areas I and II differ in terms of morphology and socio-economic characteristics, and disturbances at different time scales have varying impacts on ozone levels. However, these disturbances are likely not caused solely by meteorological factors; they also include high-frequency anthropogenic emission shocks that are synchronized with sub-hourly time scales—for example, intermittent vehicle emissions triggered by traffic signal cycles and instantaneous releases of volatile organic compounds (VOCs) during peak dining hours. Such anthropogenic perturbations can induce rapid ozone concentration fluctuations and cannot be separated from meteorological variations by the KZ filtering method alone. In particular, Monitoring Area II, as a traffic-dining composite zone, is more significantly affected by these high-frequency anthropogenic shocks, which is also an important reason for the greater dispersion of ozone concentrations observed in this area.

Pearson correlation analysis was also used to examine the meteorological factors influencing O_3 concentration changes, with the results shown in Table 5. In Area I, only half of the correlation coefficients passed the significance test at the 95% confidence level, whereas the vast majority of coefficients in area II passed. This indicates that O_3 concentrations in Area II are more strongly influenced by meteorological factors. To further analyze the degree of linear correlation between the two variables, and with reference to the classification criteria for correlation coefficients established by Zheng et al. [17], the strength of correlation was categorized as follows: strong correlation (absolute value of correlation coefficient > 0.6), moderate correlation (absolute value between 0.4 and 0.6), and weak correlation (absolute value < 0.4). As can be seen from Table 5, meteorological factors have varying effects on O_3 concentrations across different time scales and monitoring areas. For the baseline component (i.e., periods greater than 21 minutes), the direction of correlation for temperature, humidity, and radiation with O_3 concentration is consistent in both areas. Temperature and radiation show a strong correlation, while humidity exhibits a moderate correlation. This suggests that these three meteorological factors are significant contributors to O_3 concentration fluctuations. The correlations are more reliable in Area II, as most are significant at the $p<0.001$ level (indicated by ***). In contrast, wind speed shows no significant effect in Area I, but a significant, moderate negative correlation in area II. For the short-term component (i.e., variations within a period of less than 21 minutes), only wind speed showed a significant, moderate negative correlation in both areas (significant at $p<0.05$ for area I and $p<0.001$ for Area II). Solar radiation exhibited a significant, albeit weak, positive correlation, but only in Area II. The short-term effects of other factors were not significant. Therefore, it can be concluded that wind speed and solar radiation are also significant contributors to short-term O_3 concentration fluctuations. Thus, even under identical meteorological backgrounds, the effects of meteorological factors on O_3

concentration fluctuations are not entirely consistent, whether examined over long-term or short-term scales. While meteorological factors exert significant regulatory effects on O_3 variability, the confounding influence of high-frequency anthropogenic emissions cannot be ruled out. It is reasonable to infer that this inconsistency also includes other, non-meteorological factors not mentioned in the study, such as traffic and food service emissions. Consequently, the first hypothesis is fully confirmed: socio-economic factors, together with meteorological factors (temperature, humidity, solar radiation, and wind speed), exert a significantly different impact on area concentrations across different microenvironments, and this impact is also dependent on the time scale.

Regression Analysis of Ozone Variations

Multiple Linear Regression Analysis

To investigate the O_3 variation processes in Area I and Area II, an ordinary least squares (OLS) multiple linear regression model was first established as the benchmark model, and the results are presented in Table 6. The adjusted R^2 of the model is 0.3859 for Area I and 0.4725 for Area II, indicating that meteorological factors have moderate explanatory power for O_3 variations, and the explanatory power in Area II is stronger than that in Area I. In Area II, solar radiation shows a highly significant positive driving effect ($p<0.001$),

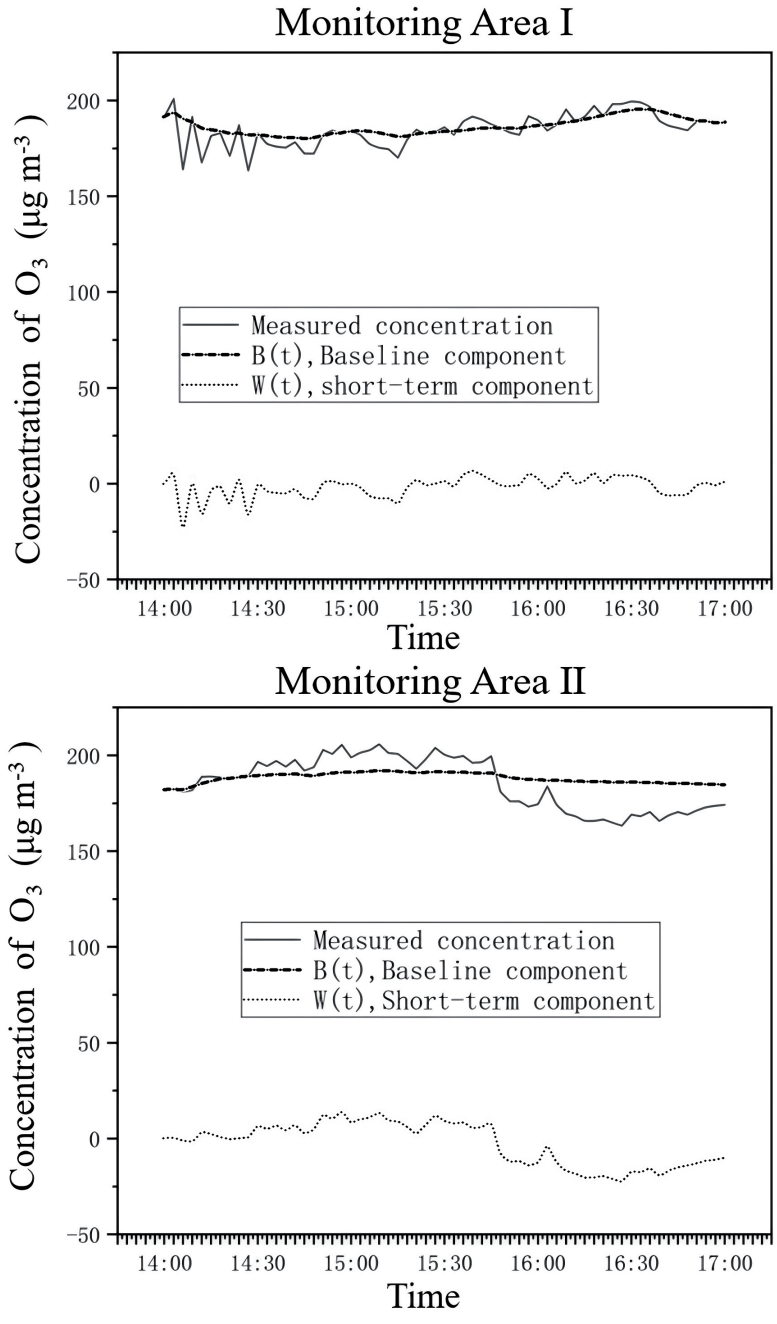


Fig. 3. Decomposition results of O_3 concentrations.

Table 4. Variance contributions for the two zones.

Monitoring Area I			Monitoring Area II		
Component	Variation (μg-² m-⁶)	Composition	Component	Variation (μg-² m-⁶)	Composition
Baseline, B(t)	83.9	19.8 %	Baseline, B(t)	85.4	22.3
Short-term, W(t)	339.7	80.2 %	Short-term, W(t)	297.8	77.7

Table 5. Correlation coefficients between O_3 concentrations and meteorological factors.

Monitoring Area I			Monitoring Area II		
Meteorological factors	Baseline component, B(t)	Short-term component, W(t)	Meteorological factors	Baseline component, B(t)	Short-term component, W(t)
Temperature	+0.71*	0.15	Temperature	+0.68***	0.12
Humidity, Radiation	-0.49*	-0.05	Humidity, Radiation	-0.45***	-0.09
Wind	+0.66*	0.11	Wind	+0.71***	+0.18*
Speed	-0.18	-0.55*	Speed	-0.23*	-0.52***
Significance: *** p<0.001; * p<0.05			Significance: * p<0.05, *** p<0.001		

and temperature shows a significant negative effect, which is consistent with the conventional understanding of ozone photochemical generation and accumulation. In Area I, temperature and relative humidity show significant positive correlations, while the independent effect of solar radiation is not significant in the presence of multicollinearity. Fig. 4 presents the OLS predictions as a straight line alongside the measured values (shown as scatter points) aligned along the same horizontal level. The predicted values increase with the observed values in both areas, indicating that the models capture the general variation in O_3 concentrations. However, the predicted values show narrower ranges than the observed values, indicating a regression-toward-the-mean effect, with high concentrations tending to be underestimated and low concentrations tending to be overestimated. The considerable dispersion around the fitted lines also suggests that additional explanatory

Table 6. Multiple linear regression results for ozone.

Monitoring Area I				
Variable	Coefficient	Std. Error	T Value	p Value
Intercept	82.0158	32.9008	2.4928	0.0157
temp	2.3851	0.9914	2.4058	0.0195
rh	0.6814	0.1501	4.5399	<0.001
rad	26.5187	16.8801	1.571	0.1218
wind	5.8528	6.7403	0.8683	0.3889

Note: Model $R^2 = 0.4268$, Adjusted $R^2 = 0.3859$, $F = 10.43 (p<0.001)$

Monitoring Area II				
Variable	Coefficient	Std. Error	T Value	p Value
Intercept	527.6173	153.4232	3.439	0.0011
temp	-10.5712	3.4242	-3.0872	0.0031
rh	-4.5007	2.9238	-1.5394	0.1293
rad	119.7525	26.9479	4.4439	<0.001
wind	-4.208	9.8109	-0.4289	0.6696

Note: Model $R^2 = 0.5077$, Adjusted $R^2 = 0.4725$, $F = 14.44 (p<0.001)$

variables or nonlinear approaches may be required to improve prediction accuracy.

Due to the strong coupling among temperature, relative humidity, and solar radiation in the afternoon monitoring period, severe multicollinearity may exist in the independent variables, which leads to coefficient inflation and unstable significance estimation in the OLS model, and reduces the reliability of quantitative inference. Therefore, multicollinearity diagnostics were carried out. The results in Table 7 show that the unstandardized condition numbers are indeed quite high, initially suggesting a serious multicollinearity issue. However, given that the raw condition numbers may be dominated by the large differences in units and scales

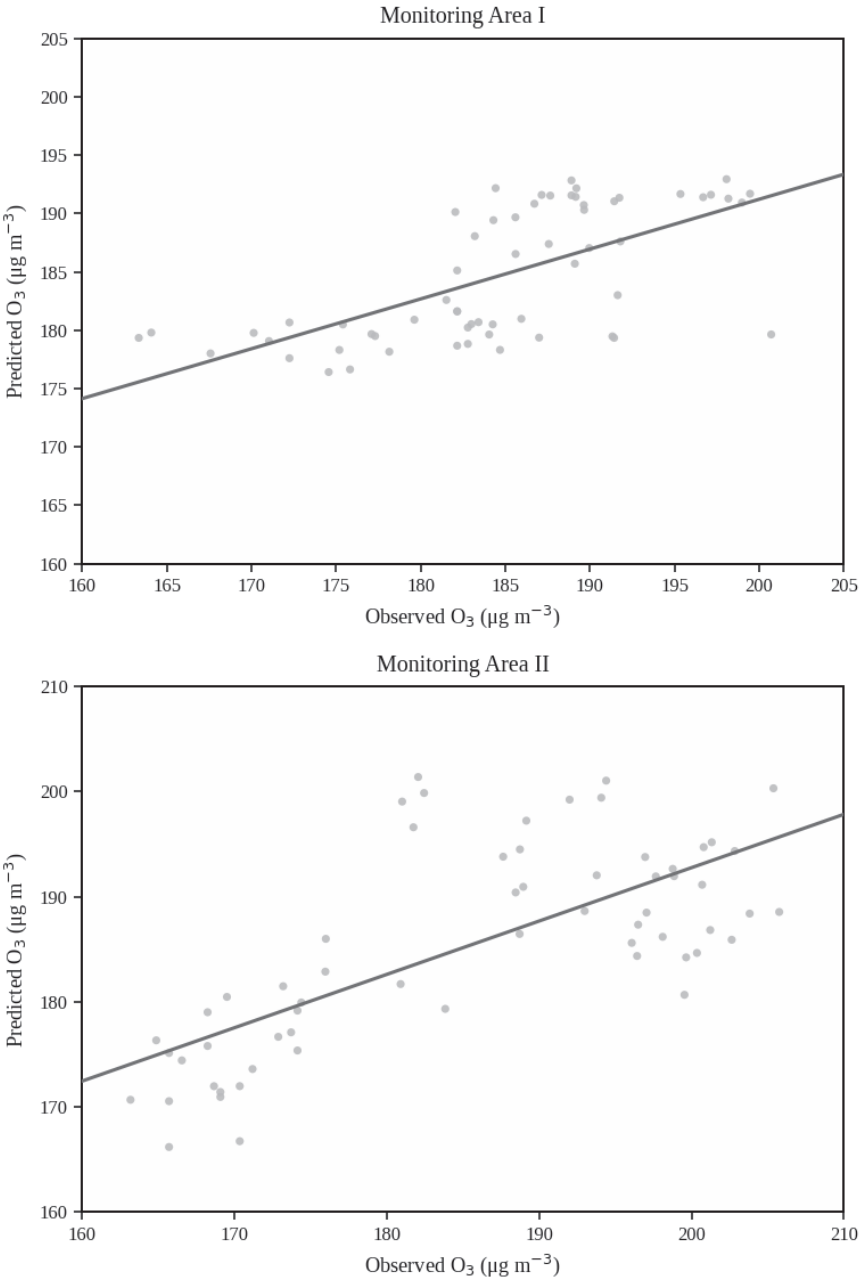


Fig. 4. Comparison of observed vs. predicted values using multiple linear regression.

Table 7. Multicollinearity diagnostics.

Metric	Area I	Area II
Condition Number	1882.7 (Unstandardized), 4.08 (Standardized)	4811.6 (Unstandardized), 4.44(Standardized)
VIF (temp/rh/rad/wind)	1.19/3.98/3.47/2.13	3.45/4.88/3.51/1.06

among the variables, all predictors were standardized to zero mean and unit variance to eliminate the influence of these scale disparities. The resulting standardized values dropped sharply (well below the conventional threshold of 30). Meanwhile, considering that some VIF values approached 5, it can be concluded that while the multicollinearity is not exceptionally severe, it should not be ignored. Therefore, it is necessary to proceed with ridge regression analysis to address the collinearity issue while providing reliable estimates of the independent effects of individual factors.

Ridge Regression Analysis

To correct multicollinearity bias, ridge regression with L2 regularization was further applied, and the optimal ridge parameter λ was determined by 10-fold cross-validation. The corrected results are shown in Table 8. After ridge regression correction, the coefficient inflation caused by multicollinearity was effectively alleviated. In Area II, the coefficient of solar radiation shrinks from 119.75 to 82.72, and all core driving factors maintain stable significance, which verifies the robustness of solar radiation as the core driving factor. In Area I, the coefficients of all variables shrink to a reasonable range as a whole. The independent effect of solar radiation is still not significant after controlling for collinearity, and the direction is slightly reversed, which reflects that under conditions of strong multi-factor coupling over short time scales, the patterns of ozone formation differ from those observed over long time periods and large spatial scales [28, 29], and the linear model cannot accurately characterize the independent effect of each factor. While ridge regression has corroborated the robustness of the key driving conclusions by mitigating multicollinearity, it does not account for the potential influence of extreme observations on the estimates. Accordingly, further verification from the standpoint of outlier resistance is warranted.

Least Absolute Deviations (LAD) Regression

To verify that the linear relationship between meteorological factors and ozone concentration is not biased by individual extreme samples, we introduced least absolute deviations (LAD) regression as a robustness check. The LAD regression results are presented in Table 9. The pseudo R^2 values are 0.2739 for Monitoring Area I and 0.3787 for Monitoring Area II, with MAE values of 4.8021 and 7.4629, respectively. In Monitoring Area I, temperature and relative humidity retain significant positive effects ($p = 0.0073$ and $p<0.001$, respectively), whereas solar radiation and wind speed are not statistically significant. In Monitoring Area II, temperature shows a significant negative effect ($p = 0.0484$), solar radiation retains a highly significant positive effect ($p<0.001$), and the effects of relative humidity and wind speed remain non-significant. These results indicate that the principal conclusions regarding the key meteorological drivers are generally robust to potential outliers. Fig. 5 shows that LAD-predicted values increase with observed values in both areas; however, the predicted ranges remain narrower than the observed ranges, indicating residual dispersion and regression toward the mean. The above analyses indicate

Table 8. Ridge regression results for ozone.

Monitoring Area I				
Variable	Coefficient	Std. Error	T Value	p Value
Intercept	171.2645	11.0257	15.5332	<0.001
temp	0.6908	0.4847	1.4251	0.1592
rh	0.1633	0.0734	2.2254	0.0298
rad	-7.8863	8.2269	-0.9586	0.3414
wind	-3.2365	3.3046	-0.9794	0.3311
Note: Optimal ridge parameter λ= 68.8138 (determined by 10-fold cross-validation); Model R^2 = 0.2910, Adjusted R^2 = 0.2404				
Monitoring Area II				
Variable	Coefficient	Std. Error	T Value	p Value
Intercept	380.2376	51.3729	7.4015	<0.001
temp	-4.9188	1.4651	-3.3574	0.0013
rh	-3.3716	1.0677	-3.1578	0.0024
rad	82.7245	12.8724	6.4265	<0.001
wind	-4.8677	6.1749	-0.7883	0.4333
Note: Optimal ridge parameter λ= 10.1394 (determined by 10-fold cross-validation); Model R^2 = 0.4709 Adjusted R^2 = 0.4331				

that while some studies have shown that improved linear models often outperform traditional ones in terms of prediction accuracy [30, 31], the meteorological-factor-based linear regression analyses, with OLS as the benchmark, still do not perform satisfactorily in terms of explanatory power and goodness-of-fit. This further

Table 9. LAD regression results for ozone.

Monitoring Area I	Variable	Coefficient	Std. Error	t Value	p Value
	const	57.1671	40.1071	1.4254	0.1596
	temp	3.3633	1.2085	2.7829	0.0073
	rh	0.6884	0.1830	3.7627	<0.001
	rad	27.0109	20.5774	1.3127	0.1947
	wind	8.0182	8.2166	0.9759	0.3333
	Note: Pseudo R^2 = 0.2739; MAE = 4.8021; RMSE = 6.5181				
Monitoring Area II	Variable	Coefficient	Std. Error	t Value	p Value
	const	401.6054	208.7194	1.9241	0.0594
	temp	-9.4002	4.6583	-2.0180	0.0484
	rh	-1.8865	3.9775	-0.4743	0.6371
	rad	157.8122	36.6603	4.3047	<0.001
	wind	1.0500	13.3470	0.0787	0.9376
	Note: Pseudo R^2 = 0.3787; MAE = 7.4629; RMSE = 9.6021				

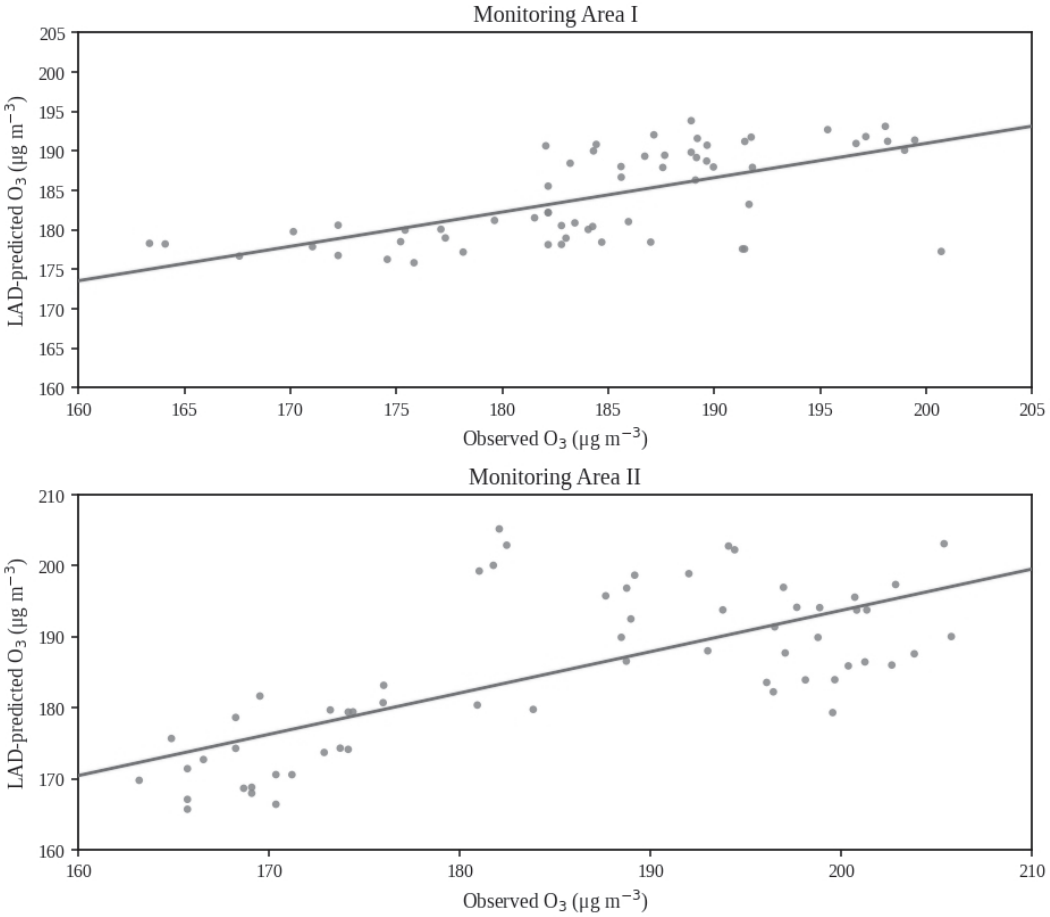


Fig. 5. Comparison of observed vs. predicted values using LAD regression.

confirms the limitations of the linear hypothesis in characterizing ozone dynamics in micro-environmental settings and reinforces the necessity of conducting subsequent nonlinear analyses using GAM.

GAM Model Analysis

The model results (shown in Table 10) indicate that the explanatory power (pseudo R^2) of the model for O_3 concentrations reached 0.580 and 0.794 for monitoring Area I and area II, respectively. This shows that the four meteorological variables alone can explain approximately 58% and 79% of the O_3 variation in Area I and Area II, respectively. This explanatory power is significantly higher than that of both the multiple linear regression and the minimum-area regression analyses. These findings are largely consistent with previous studies that applied multivariate GAM analysis to urban ozone in similar settings [32, 33]. However, the relationship between O_3 variation and the four meteorological factors appears to be even stronger in Area II. The AIC, AICc, and GCV values for both zones indicate that the models have a good fit and good generalization performance. All smooth terms (s(temp), s(rh), s(rad), s(wind)) were significant at the $p<0.001$ level, indicating that temperature, relative humidity, solar radiation, and wind speed all exert significant nonlinear effects on O_3 concentrations. The effective degrees of freedom (EDF) for all smooth terms are approximately 20, which is significantly greater than 1, suggesting that a linear assumption cannot capture the ozone response driven by meteorological factors, confirming the complex nonlinear effects of these factors. The scale parameter (σ^2) increased from 45.33 in area I to 54.33 in Area II, which implies that, in addition to meteorology, other localized source and sink processes not included in the model (such as emissions from traffic and food service) are having an effect in Area II. This finding, in turn, provides further confirmation of a key aspect of the first hypothesis: that socio-economic factors, together with meteorological factors, influence ozone concentrations.

To visualize the nonlinear effects of meteorological factors on O_3 more intuitively, Fig. 6 presents the partial dependence curves for the four meteorological variables from the GAM for Monitoring Area I. The curves show that the deviation in O_3 concentration from the model intercept, caused by changes in each meteorological factor, is not uniform, indicating significant nonlinearity, which is consistent with the previous findings. Among these, the fluctuations caused by the meteorological factors are more pronounced in Area II. However, the influence of low humidity and high solar radiation is more significant in Area I.

To ensure the quality and reliability of the developed GAM, the model fit was further validated using multiple methods, as shown in Fig. 7. In Area I, the histogram of residuals is slightly right-skewed but still approximately normal. In Area II, the residual values most frequently occur near zero. Both findings are generally consistent with the GAM's assumption of normality. The residual-versus-fitted value plot shows no clear funnel shape or curved pattern, indicating that the assumption of homoscedasticity is largely met. In the Q-Q plot, the tails of area I deviate slightly from the diagonal, while the deviation is even smaller for Area II. These deviations are acceptable, and the normality assumption is deemed satisfactory. In summary, the model demonstrates good statistical reliability and is suitable for analyzing the influence of meteorological factors on ozone.

Correlation of Meteorological Factors

Although the WBGT index in this study was obtained through instrumental measurements, the relationship between ambient temperature, humidity, solar radiation intensity, and WBGT can generally be examined using the calculation method. However, the relationship between wind speed and WBGT

Table 10. GAM fitting results.

	Smooth Term	EDF	p-value
Monitoring area I	s(temp)	19.99	< 0.001
	s(rh)		
	s(rad)		
	s(wind)		
	Pseudo R^2 = 0.58; AIC = 620.29; AICc = 643.96;GCV = 104.04; σ^2 = 45.33		
	Smooth Term	EDF	p-value
Monitoring area II	s(temp)	19.77	< 0.001
	s(rh)		
	s(rad)		
	s(wind)		
	Pseudo R^2 = 0.794;AIC = 641.70; AICc = 664.61; GCV = 122.67; σ^2 = 54.33.		

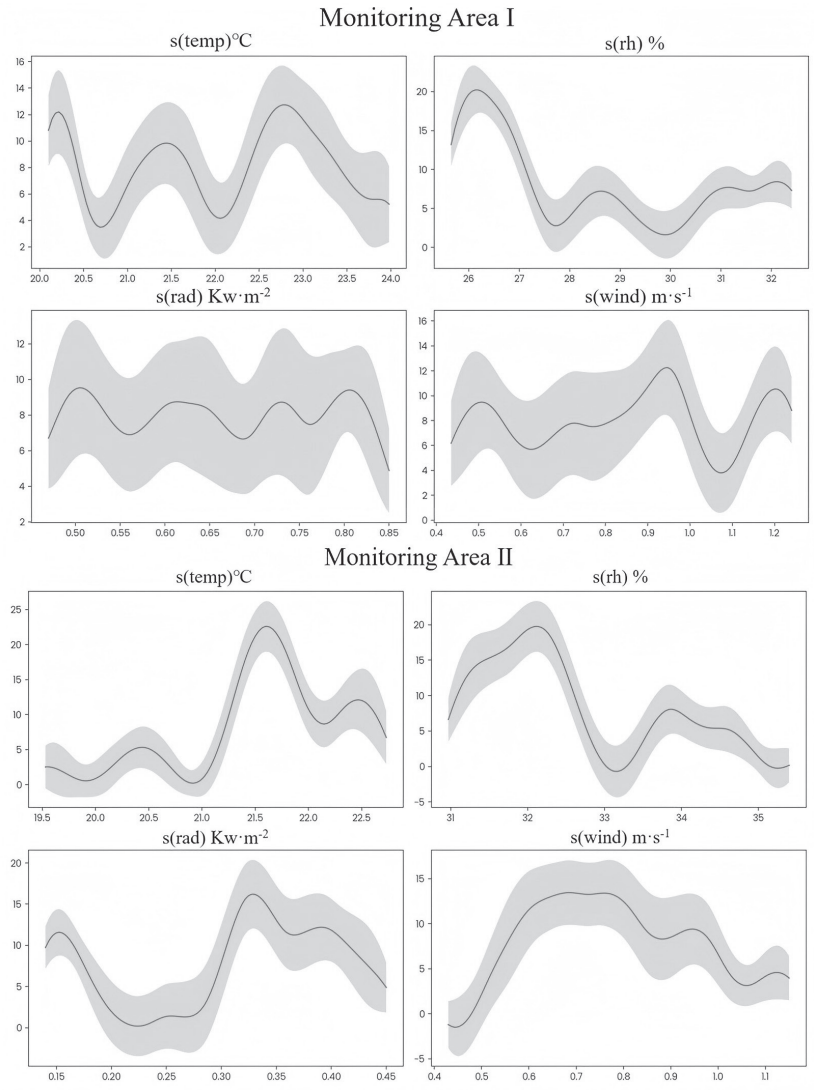


Fig. 6. Partial dependence curves for the meteorological variables in the GAM (the shaded areas represent the 95% confidence intervals).

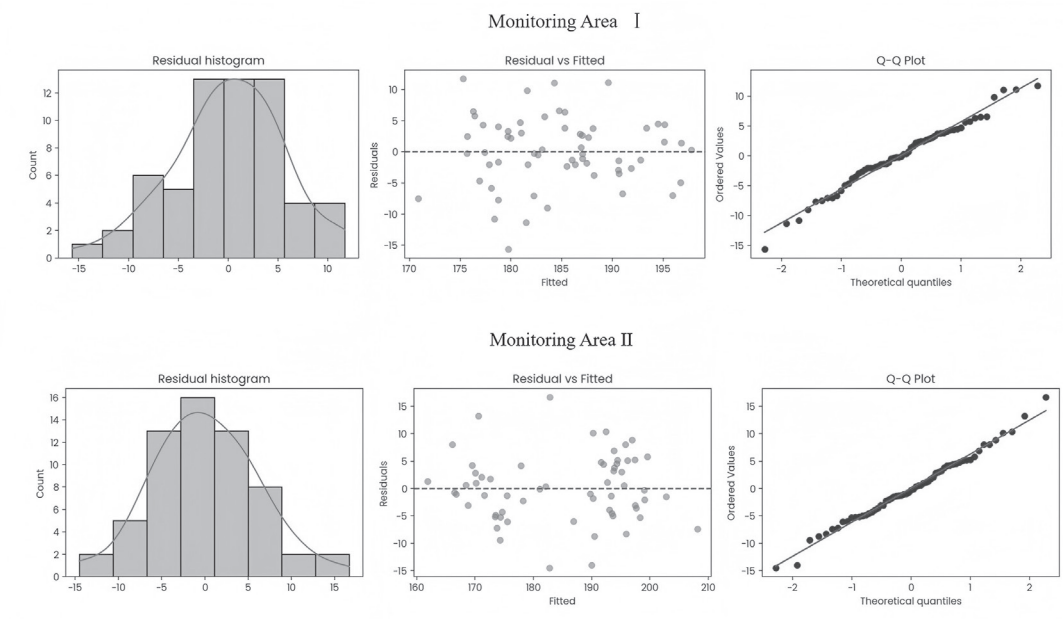


Fig. 7. GAM residual diagnostics. a) Histogram of residuals; b) Residuals vs. fitted values; c) Q-Q plot.

Table 11. Correlation of meteorological factors.

Monitoring Area I		Temp	rh	rad	wind
	temp	1.00	-0.77	-0.23	-0.24
	rh	-0.77	1.00	0.75	0.60
	rad	-0.23	0.75	1.00	0.64
	wind	-0.24	0.60	0.64	1.00
		Temp	rh	rad	wind
Monitoring Area II	temp	1.00	-0.84	0.76	-0.18
	rh	-0.84	1.00	-0.84	0.16
	rad	0.76	-0.84	1.00	-0.22
	wind	-0.18	0.16	-0.22	1.00

remains unclear, necessitating a targeted analysis. The correlation analysis results show that in Area I, the correlation coefficient between the two was 0.07, indicating an almost negligible linear relationship. In Area II, the coefficient was -0.2, showing a very weak negative correlation. This suggests that wind speed did not have a significant impact on temperature, humidity, or irradiance. This is likely closely related to the fact that the wind speed during this study was not high and exhibited little variation.

A correlation analysis of the four meteorological factors was then conducted to further elucidate their roles. As shown in Table 11, temperature, relative humidity, and solar radiation exhibited strong correlations with each other in both areas, whereas wind speed showed relatively weak correlations with the other three factors. In both Areas I and II, temperature and humidity demonstrated a strong negative correlation. In Area II, temperature and radiation intensity showed a strong positive correlation, while relative humidity and radiation intensity exhibited a very strong negative correlation. Therefore, the presence of collinearity among the aforementioned four factors was once again confirmed.

Compensatory Relationship

Maintaining atmospheric environmental quality requires appropriate WBGT levels and stable, compliant ozone concentrations. Therefore, the compensatory mechanism can be inferred from the apparent relationship between the two indicators, or it can be deduced from a more intrinsic or detailed perspective. An examination of the apparent correlation between the two indicators reveals a very weak relationship, which indicates that ozone pollution and the thermal environment indicator indeed belong to different categories, making it infeasible to directly extract a compensatory mechanism based solely on their apparent relationship. However, from an intrinsic or detailed perspective, since both of these indicators are closely related to meteorological factors, the relationship between them should, in fact, be significant. Consequently, by adjusting the meteorological factors, both indicators will change accordingly, allowing the regulatory patterns needed to meet the different indicator requirements to be derived from this relationship. To ensure that the compensation framework aligns with regulatory requirements and practical microenvironmental management needs, the tiered classification of O_3 concentrations is established based on the Chinese National Ambient Air Quality Standard (GB 3095-2026). According to this standard, the hourly average O_3 concentration limits are 160 $\mu g \cdot m^{-3}$ for Grade I and 200 $\mu g \cdot m^{-3}$ for Grade II (applicable to urban residential, commercial, and traffic zones, including the study area). To achieve refined regulation under compliance conditions, and given that the majority of O_3 observations in this study fall within the transition range between Grade I and Grade II, the O_3 concentrations not exceeding the hourly standard (200 $\mu g \cdot m^{-3}$) were divided into five tiers. For each tier, WBGT was linearly regressed against the corresponding temperature, relative humidity, solar radiation, and wind speed. The results are shown in Fig. 8. These two figures illustrate the adjustment strategies for temperature, humidity, solar radiation intensity, and wind speed required to maintain the five tiers of sub-standard ozone concentrations and their corresponding WBGT levels (all WBGT values obtained in this study were within the relevant standard limits), within the range of factor values covered by this research. For example, in area I, if the O_3 concentration is between 163.087 and 171.247 $\mu g\ m^{-3}$, it falls under Tier 1 in Fig. 8. According to the linear regression equation for Tier 1 in the figure, for every one-unit increase in WBGT, the temperature must increase by approximately 1.4°C, relative humidity must decrease by 4.1%, solar radiation must decrease by 0.28, and wind speed must decrease by 0.24. Conversely, a decrease in temperature of 1.4°C, along with increases of 4.1% in humidity, 0.28 in solar radiation, and 0.24 in wind speed, would maintain a stable WBGT. These adjustments can be implemented through measures

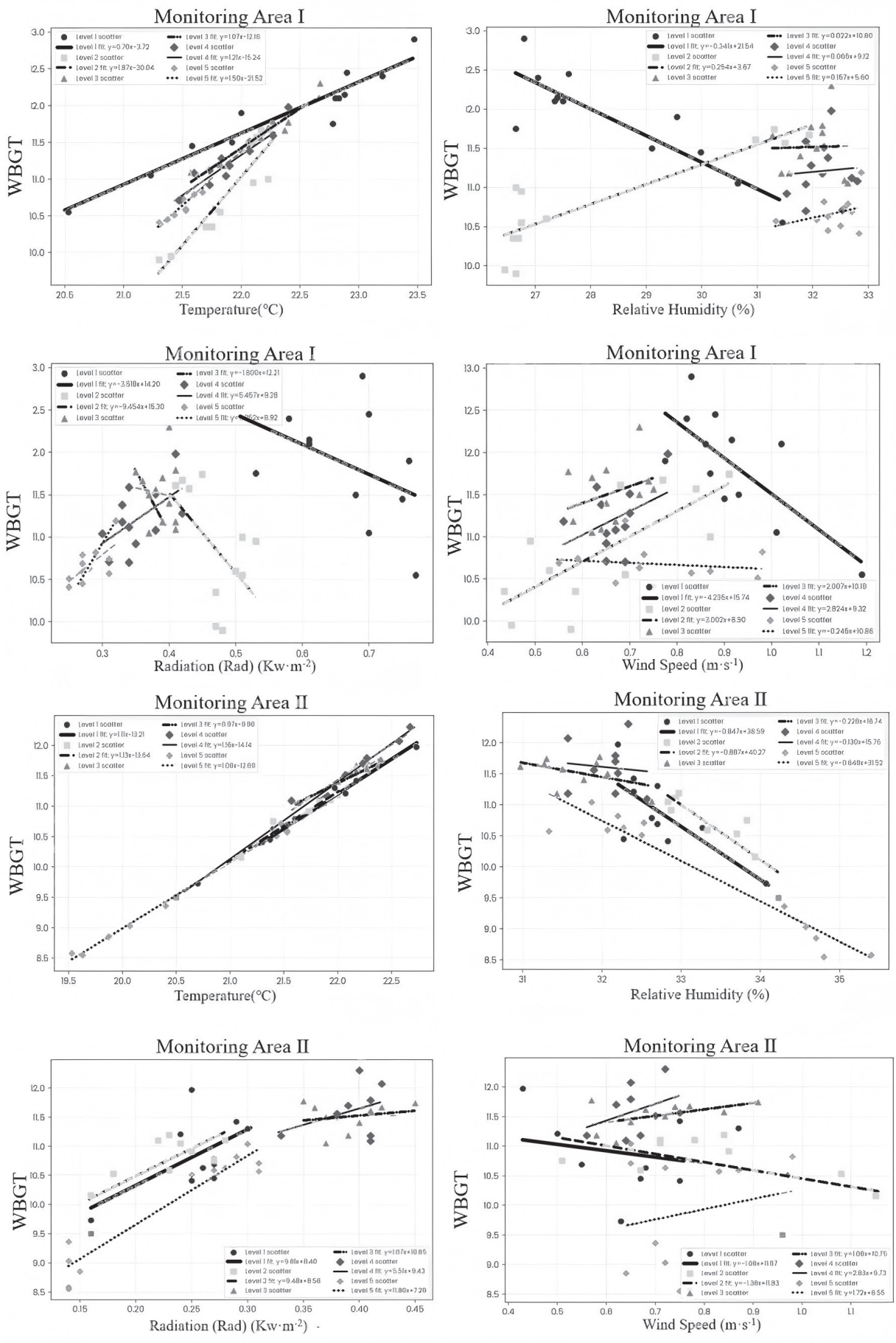


Fig. 8. Patterns of meteorological factor variations for maintaining ozone concentration and WBGT.

aimed at improving microenvironmental conditions, such as enhancing ventilation, optimizing vegetation coverage, and introducing air humidification. Although this method is not highly precise, it can generally meet the requirements for outdoor work. Consequently, the second hypothesis is successfully validated. Namely, a potential connection, linked via meteorological factors, exists between WBGT and ozone concentration, and this connection allows a compensatory mechanism to be identified through zoned regression analysis under specific scenarios. Moreover, from a macro viewpoint that incorporates environmental regulations and socioeconomic factors, prior research has shown that environmental policies should not be driven solely by pollution reduction, but must also weigh multiple competing goals, including ecological security, social equity, and economic sustainability [34]. This study serves as a technical complement to that perspective. While existing work on the co-control of heat stress and pollutants – such as the effects of streets and vegetation [35, 36] – has been largely static, our study provides a distinctive technical angle by examining the compensatory interplay among microscale meteorological variables.

Conclusions

In summary, this research not only deepens the understanding of the factors influencing O_3 and WBGT in two typical urban street microenvironments under non-typical meteorological conditions, but also, for the first time from a multiscale perspective, reveals the synergistic regulatory logic between air pollution and thermal comfort, and validates two core hypotheses. First, the study confirms that even outside the typical hot and humid ozone-forming seasons, meteorological factors exert a significant multiscale and microenvironment-heterogeneous impact on O_3. KZ decomposition results indicate that short-term fluctuations dominate the total O_3 variance, with wind speed emerging as a key suppressor of O_3 at sub-hourly scales. At baseline scales, solar radiation and temperature positively drive O_3, while humidity exhibits a negative influence – effects that are more pronounced in the "traffic-dining" zone. In both types of urban microenvironments, certain coupling relationships exist among meteorological factors. After ridge regression correction, the coefficient directions and significance levels remained broadly stable, confirming that solar radiation (positively driving Area II) and temperature (positively in Area I, negatively in Area II) serve as the core driving factors. The LAD regression further corroborated that these key conclusions are not biased by extreme samples, demonstrating good robustness. However, the explanatory power of the linear models remains limited, and they struggle to accurately capture extreme concentration values. GAM analysis further reveals strong nonlinear relationships between all meteorological factors and O_3, indicating that linear models are insufficient to capture their complex interactions. Moreover, the higher residual variance in the model for Monitoring Area II suggests that anthropogenic emissions, such as vehicle exhaust and cooking-related VOCs, play an important role in local O_3 dynamics, highlighting how socioeconomic context and micro-morphology jointly shape pollution patterns. Second, the study successfully verifies that although O_3 and WBGT belong to different environmental dimensions, they are intrinsically coupled through shared meteorological drivers, offering potential for co-optimization. Zoned regression analysis demonstrates that within different below-standard O_3 concentration ranges, targeted adjustment of temperature, humidity, solar radiation, and wind speed can regulate WBGT levels accordingly. This finding provides an actionable compensatory pathway for fine-grained microenvironment management aimed at the dual objectives of "pollution control and thermal comfort enhancement". Future urban climate adaptation planning urgently needs to incorporate high-frequency, fine-resolution microenvironment monitoring systems and develop integrated intervention strategies that combine meteorological regulation, spatial design, and emission management, so as to tangibly enhance the resilience and livability of urban habitats. It should be noted, however, that the findings of this study are primarily applicable to microenvironmental conditions during clear-sky afternoons. Future work should expand to include all-weather, multi-day monitoring and contributions from high-frequency anthropogenic emissions.

Acknowledgments

The authors acknowledge the work conducted by a graduate student (Ren Jing) and the resources and facilities provided by the University of Electronic Science and Technology of China, Zhongshan Institute and the Science and Technology Innovation Project of the Department of Housing and Urban-Rural Development of Guangdong Province.

Conflict of Interest

The authors declare no conflict of interest.

AI Usage Disclosure Statement

During the preparation of this work, the authors used KIMI-K3 for English language editing and for the adjustment of figure colour schemes. After using this tool, the authors reviewed and edited the content as needed and take full responsibility for the content of the publication.

References

1. TAUBENBÖCK H., MAST J., GEISS C., WURM M., ESCH T., SETO K.C. Global differences in urbanization dynamics from 1985 to 2015 and outlook considering IPCC climate scenarios. Cities, **151**, 105117, **2024**.
2. BARUTI M.M., YAHIA M.W., JOHANSSON E. Spatial and temporal variations of microclimate and outdoor thermal comfort in informal settlements of warm humid Dar es Salaam, Tanzania. Heliyon, **10** (1), e23160, **2024**.
3. SLIMI K., CHROUDA A., ÖZTOP H.F. Traffic effects on global warming: A review. Renewable and Sustainable Energy Reviews, **226** (Part A), 116248, **2026**.
4. ROY T.B., MIDDEY A., KRUPADAM R.J. Unveiling the microclimate: A comprehensive review of tools, techniques, and future directions for sustainable cities. Building and Environment, **274**, 112726, **2025**.
5. MANAPRAGADA N.V.S.K., NATANIAN J. Urban Microclimate and Energy Modeling: A Review of Integration Approaches. Sustainability, **17** (7), 3025, **2025**.
6. RAPTI T., KANTZIOURA A. Study of urban microclimate conditions in a commercial area of an urban centre and the environmental regeneration potential. IOP Conference Series: Earth and Environmental Science, **899**, 012017, **2021**.
7. CORRÊA M.P., BASTOS I.R.P., YAMAMOTO A.L.C. A global score for skin environmental exposure: integrating UV radiation, heat, and pollution via fuzzy analytic hierarchy process. International Journal of Biometeorology, **70** (4), 117, **2026**.
8. ABERA T.A., MAEDA E.E., HEISKANEN J., WÖLLAUER S., ALIBAKHSHI S., PELLIKKA P., HEMP A., MORADI A., HAILU B.T., MUHAMMED M.A., ZEUSS D. Deforestation reduces microclimate buffering of African montane forests. Communications Earth & Environment, **6** (1), 877, **2025**.
9. BRANKOVIC M.D., IGIC M., DEKIC J., LJUBENOVIC M. Impact of Urban Densification on Outdoor Microclimate and Design of Sustainable Public Open Space in Residential Neighborhoods: A Study of Niš, Serbia. Sustainability, **17** (4), 1573, **2025**.
10. KISVARGA S., HOROTÁN K., PUSZTAHELYI T., BORONKAY G., ISTVÁNFI Z., OROSZ V., ALMÁSI C., ORLÓCI L. When quiet streets are more toxic: The paradox of low-traffic urban canyons. Urban Forestry & Urban Greening, **120**, 129445, **2026**.
11. GREENSLADE M., GUO Y., BETITO G., MIRREZAEI M.A., ROYCHOUDHURY C., ARELLANO A.F., SOROOSHIAN A. On ozone's weekly cycle for different seasons in Arizona. Atmospheric Environment, **334**, 120703, **2024**.
12. ITAHASHI S., SHIMADERA H., IRIE H., KITAYAMA K., CHATANI S. Changes in ambient ozone concentrations from urban to remote areas in Japan during the COVID-19 pandemic period in April and May, 2020. Progress in Earth and Planetary Science, **13** (1), 5, **2026**.
13. IRMAK M.A., BILGE C., YILMAZ S., DAS M.E. Microclimate-focused thermal comfort assessment in coastal settlements with tourism activities. Pure and Applied Geophysics, **182**, 2199, **2025**.
14. ARSISO B.K. Urban land cover transformations and thermal dynamics through integrated LULC, UHI, and ecological vulnerability assessment using remote sensing indices in the City of Addis Ababa, Ethiopia. Sustainable Cities and Society, **135**, 107017, **2025**.
15. STOCKWELL C.E., COGGON M.M., SCHWANTES R.H., HARKINS C., VERREYKEN B., LYU C., ZHU Q., XU L., GILMAN J.B., LAMPLUGH A., PEISCHL J., ROBINSON M.A., VERES P.R., LI M., ROLLINS A.W., ZURASKI K., BAIDAR S., LIU S., KUWAYAMA T., BROWN S.S., MCDONALD B.C., WARNEKE C. Urban ozone formation and sensitivities to volatile chemical products, cooking emissions, and NOx upwind of and within two Los Angeles Basin cities. Atmospheric Chemistry and Physics, **25** (2), 1121, **2025**.
16. KAZEMI A., CIRELLA G.T., HEDAYATIAGHMASHHADI A., GILI M. Temporal-spatial distribution of surface urban heat island and urban pollution island in an industrial city: Seasonal analysis. IEEE Journal of Selected Topics in Applied Earth Observations and Remote Sensing, **18**, 7100, **2025**.
17. LI Y., LI L., XIE J. Study on variation characteristics of O_3 at different time scales in Shaoguan city based on KZ filter method. Acta Scientiae Circumstantiae, **43** (1), 128, **2023** [In Chinese].
18. ZHENG X., LI M., LOU P. Different-scale changes in ozone concentration and meteorological environment in Fenwei Plain. Plateau Meteorology, **40 (**4), 954, **2021** [In Chinese].
19. THOMPSON A.M., STAUFFER R.M., KOLLONIGE D.E., ZIEMKE J.R., JOHNSON B.J., MORRIS G.A., CULLIS P., CAZORLA M., DIAZ J.A., PITERS A., NEDELJKOVIC I., WARSODIKROMO T., RAIMUNDO SILVA F., NORTHAM E.T., BENJAMIN P., MKOLOLO T., MACHININI T., FÉLIX C., ROMANENS G., NYADIDA S., BRIOUDE J., EVAN S., METZGER J.M., DINDANG A., MAHAT Y.B., SAMMATHURIA M.K., ZAKARIA N.B., KOMALA N., OGINO S.Y., QUYEN N.T., MANI F.S., VUIYASAWA M., NARDINI D., MARTINSEN M., KUNIYUKI D.T., MÜLLER K., WOLFF P., SAUVAGE B. Tropical tropospheric ozone trends (1998 to 2023): new perspectives from SHADOZ, IAGOS and OMI/MLS observations. Atmospheric Chemistry and Physics, **25** (24), 18475, **2025**.
20. BOGNAR K., TEGTMEIER S., BOURASSA A., ROTH C., WARNOCK T., ZAWADA D., DEGENSTEIN D. Stratospheric ozone trends for 1984-2021 in the SAGE II–OSIRIS–SAGE III/ISS composite dataset. Atmospheric Chemistry and Physics, **22**, 9553, **2022**.
21. OMARA T M. Ridge and Liu-Type Estimators for Tobit SUR Model: Application to Air pollution Data. Journal of Multidisciplinary Applied Natural Science, **6** (2), 1011, **2026**.
22. LI Y., DANIELACHE S. O., NANBU S., UENO Y. CS_2 absorption cross-sections measurement in 280-360 nm region using least absolute deviation method. Journal of Quantitative Spectroscopy and Radiative Transfer, **345**, 109569, **2025**.
23. BOLETI E., HUEGLIN C., TAKAHAMA S. Trends of surface maximum ozone concentrations in Switzerland based on meteorological adjustment for the period 1990-2014. Atmospheric Environment, **213**, 326, **2019**.
24. BOLETI E., HUEGLIN C., GRANGE S.K., PRÉVÔT A.S.H., TAKAHAMA S. Temporal and spatial analysis of ozone concentrations in Europe based on timescale decomposition and a multi-clustering approach. Atmospheric Chemistry and Physics, **20** (14)**,** 9051, **2020**.
25. JIANG Y., ZHU A., JIANG S., LI Z., YANG C. Evaluation of O_3 and NOx pollution based on people's perception. Polish Journal of Environmental Studies, **31** (1), 979, **2022**.

26. REDI T., YOHANNES H. Assessing Air Quality Variation Focusing on Criteria Pollutants in Metropolitan City, Addis Ababa, Ethiopia. Advances in Meteorology, **2026** (1), 7668731, **2026**.
27. FARDILAH R.D., TURYANTI A., PANGESTU L.A., DOMINICA M.V., Perdinan. Systematic literature review on ozone dispersion correlated with diurnal concentration pattern in urban and rural areas. Agromet, **37** (2), 77, **2023**.
28. TRÁJER A.J., NAGY G., DOMOKOS E. Exploration of the heterogeneous effect of climate change on ozone concentration in an urban environment. International Journal of Environmental Health Research, **29** (3), 276**, 2019**.
29. MISHRA M., BOOPATHY R., MALLIK C., DAS T. Particulate/gaseous pollutants and solar radiation fluctuations over Bhubaneswar amidst two special events: Diwali and solar eclipse. Atmospheric Pollution Research, **15** (7), 102117, **2024**.
30. ALSHAHRANI F., FETITAH O., ALMANJAHIE I.M., ATTOUCH M.K. Spatiotemporal Analysis of Ozone Concentration Using Semi-Functional Partial Linear Models. Chiang Mai Journal of Science, **50** (6), e2023075, **2023**.
31. GHAHREMANLOO M., CHOI Y., LOPS Y. Deep learning mapping of surface MDA8 ozone: The impact of predictor variables on ozone levels over the contiguous United States. Environmental Pollution, **326**, 121508, **2023**.
32. TUDOR C., HOROBET A., SOVA R., BELASCU L., PENTESCU A. Decoding Urban Traffic Pollution: Insights on Trends, Patterns, and Meteorological Influences for Policy Action in Bucharest, Romania. Atmosphere, **16** (8), 916, **2025**.
33. SANTRA S., PATRA A., ALAM G., PENCHALA A. Ozone Variability Induced by Meteorological Factors and Precursors During Pre- and Post-Monsoon Periods. Ozone: Science & Engineering, **48** (2), 225, **2026**.
34. ZHAO W., TOH M.Y., ZHANG Y. The price of green justice: Environmental courts and cross-regional capital immobility. Finance Research Letters, **85** (Part A), 107883, **2025**.
35. SCHAEFER M., SALARI H.E., KÖCKLER H., THINH N.X. Assessing local heat stress and air quality with the use of remote sensing and pedestrian perception in urban microclimate simulations. Science of the Total Environment, **794**, 148709, **2021**.
36. MONDANELLI L., FRANCINI S., PASSARINO L., SALBITANO F., SPEAK A., CHIRICI G., COCOZZA C. Coupling remote sensing data and local meteorological measurements to predict thermal stress and its potential mitigation by urban forests. Urban Forestry & Urban Greening, **113**, 129113, **2025**.